

ARTICLE



Myxoid pleomorphic liposarcoma is distinguished from other liposarcomas by widespread loss of heterozygosity and significantly worse overall survival: a genomic and clinicopathologic study

Josephine K. Dermawan¹, Sinchun Hwang², Leonard Wexler³, William D. Tap³, Samuel Singer⁴, Chad M. Vanderbilt^{1,5} and Cristina R. Antonescu^{1,5}

© The Author(s), under exclusive licence to United States & Canadian Academy of Pathology 2022

Myxoid pleomorphic liposarcoma (MPLPS) is a recently described and extremely rare subtype of liposarcoma with a predilection for the mediastinum. However, the genomic features of MPLPS remain poorly understood. We performed comprehensive genomic profiling of MPLPS in comparison with pleomorphic liposarcoma (PLPS) and myxoid/round cell liposarcoma (MRLPS). Of the 8 patients with MPLPS, 5 were female and 3 were male, with a median age of 32 years old (range 10–68). All except one were located in the mediastinum, with invasion of surrounding anatomic structures, including chest wall, pleura, spine, and large vessels. All cases showed an admixture of morphologies reminiscent of PLPS and MRLPS, including myxoid areas with plexiform vasculature admixed with uni- and/or multivacuolated pleomorphic lipoblasts. Less common features included well-differentiated liposarcoma-like areas, and in one case fascicular spindle cell sarcoma reminiscent of dedifferentiated LPS. Clinically, 4 experienced local recurrence, 4 had distant metastases and 5 died of disease. Compared to PLPS and MRLPS, patients with MPLPS had worse overall and progression-free survival. Recurrent *TP53* mutations were present in all 8 MPLPS cases. In contrast, in PLPS, which also showed recurrent *TP53* mutations (83%), *RB1* and *ATRX* losses were more common. MRLPS was highly enriched in *TERT* promoter mutations (88%) and PI3K/AKT pathway mutations. Copy number profiling in MPLPS revealed multiple chromosomal gains with recurrent amplifications of chromosomes 1, 19 and 21. Importantly, allele-specific copy number analysis revealed widespread loss of heterozygosity (80% of the genome on average) in MPLPS, but not in PLPS or MRLPS. Our findings revealed genome-wide loss of heterozygosity co-existing with *TP53* mutations as a characteristic genomic signature distinct from other liposarcoma subtypes, which supports the current classification of MPLPS as a stand-alone pathologic entity. These results further expand the clinicopathologic features of MPLPS, including older age, extra-mediastinal sites, and a highly aggressive outcome.

Modern Pathology (2022) 35:1644–1655; <https://doi.org/10.1038/s41379-022-01107-6>

INTRODUCTION

Myxoid pleomorphic liposarcoma (MPLPS) is an extremely rare liposarcoma subtype with a predilection for the mediastinum. Among the few case series published thus far, MPLPS mostly occurs in young adults (<30 years old) with a female predominance. MPLPS has a high recurrence rate and poor overall survival^{1,2}. Morphologically, as the name implies, MPLPS shows a variable proportion of myxoid/round cell liposarcoma (MRLPS)-like areas, including plexiform vasculature and pulmonary edema-like myxoid pools and more cellular, and high-grade pleomorphic liposarcoma (PLPS)-like areas with pleomorphic lipoblasts and increased cytological atypia^{1–3}.

In terms of molecular findings, MPLPS lack *FUS/EWSR1-DDIT3* gene fusions and *MDM2/CDK4* amplifications^{1,2}. Although

recurrent genomic alterations have not been well defined in MPLPS, studies have demonstrated complex chromosomal alterations including gains involving chromosomes 1, 6–8, 18–21 and losses involving chromosomes 2–5, 10–17, and 22^{3,4}. Some studies have identified losses in 13q14, which encompassed *RB1*, in a subset of cases^{3,5}. One case report revealed a hyperdiploid/hypotriploid karyotype derived from a near haploid genome via SNP array⁵. Unsupervised clustering on methylation profiling revealed a possible relationship of MPLPS to PLPS but not MRLPS³.

In this study, using comprehensive genomic profiling of mutations, copy number alterations, and allele-specific copy number, we aim to define the characteristic genomic features of MPLPS in comparison to its close morphologic mimics, PLPS and MRLPS.

¹Department of Pathology and Laboratory Medicine, Memorial Sloan Kettering Cancer Center, New York, NY, USA. ²Department of Radiology, Memorial Sloan Kettering Cancer Center, New York, NY, USA. ³Department of Medicine, Memorial Sloan Kettering Cancer Center, New York, NY, USA. ⁴Department of Surgery, Memorial Sloan Kettering Cancer Center, New York, NY, USA. ⁵These authors contributed equally: Chad M. Vanderbilt, Cristina R. Antonescu. ✉email: antonesc@mskcc.org

Received: 25 March 2022 Revised: 6 May 2022 Accepted: 6 May 2022

Published online: 7 June 2022

MATERIALS AND METHODS

Case selection and study cohort

After approval from the Institutional Review Board, cases were identified from the Memorial Sloan Kettering Cancer Center (MSKCC) surgical pathology archives from 2013 to 2021. Criteria included cases with an explicit diagnosis of “myxoid pleomorphic liposarcoma”, or (pleomorphic) liposarcoma cases that occur in the mediastinum or head and neck area and fulfill the morphologic criteria of MPLPS: harboring a combination of areas characteristic of MLPS and those of PLPS on manual review. We excluded liposarcomas from the extremities, particularly the thighs, to avoid inclusion of conventional PLPS into our MPLPS cohort. Additionally, to avoid including cases of well-differentiated/dedifferentiated liposarcoma and MRLPS, any cases with *MDM2* amplification or *DDIT3* rearrangements were excluded from the MPLPS cohort. For myxoid/round cell liposarcoma (MRLPS), only molecularly confirmed cases, either *DDIT3* rearrangement by fluorescence in situ hybridization (FISH) or *FUS/ESR1::DDIT3* fusion by Archer testing, were included. High-grade MRLPS was defined as the presence of round cell component greater than or equal to 5%. None of the MRLPS and PLPS cases included in the control group were located in the mediastinum or head and neck.

Targeted DNA sequencing

Detailed descriptions of MSK-IMPACT workflow and data analysis, a hybridization capture-based targeted DNA NGS assay for solid tumor were described previously⁶.

Copy number and mutational profiling and data analysis

Data analysis was performed using R version 4.1.0. MSK-IMPACT data were imported using R packages “gnomeR” version 1.0.0 and “cBioportalR” version 0.0.0.9000. Mutations and gene-level copy number alterations were visualized and summarized using the oncoplot function of the R package “maftools” version 2.8.5⁷. Cohort level copy number profiles and segmentations was derived using the reduced segmentation function of R package “CNTools” version 1.48.0⁸. Copy number profiles were visualized using “sigminer” version 2.1.2⁹, and “circlize” version 0.4.13¹⁰.

Allele-specific copy number analysis was performed using the Fraction and Copy number Estimate from Tumor/normal Sequencing (FACETS) algorithm with R package “facets” version 0.6.2¹¹. Since FACETS analysis requires matched tumor-normal pair to cancel out mapping bias, only 7 out of 8 MPLPS samples (cases 2–8) were subjected to FACETS analysis. Allele imbalance [loss of heterozygosity (LOH)] was determined by the allele log-odds-ratio (logOR), which is defined by the log-odds-ratio of the variant allele read count of heterozygous single nucleotide polymorphism (SNP) sites in the tumor versus in the normal. Where possible, the diploid state (diplogR) was manually reviewed and optimized by referencing chromosomal segments that are presumed to best approximate a diploid state [total copy number (tcn) = 2, lesser (minor) copy number (lcn) = 1, no loss of heterozygosity (LOH)]. In cases with whole genome LOH, the tumors lack of any diploid chromosomal segments and thus the most common diplogR state is selected for the remaining analysis. The percentage LOH across the genome for each sample was calculated by dividing the total lengths of segments with LOH (logOR > 0.5) by the total lengths of all segments using the FACETS segmentation results from the expectation-maximization (EM) fit output.

Survival analysis

Survival analysis by comparison of hazard ratios using log rank *P* testing and visualization of Kaplan-Meier curves were performed using R packages “survminer” version 0.4.9 and “survival” version 3.2.13. Clinical charts were manually reviewed to document date of initial presentation, disease progression, and survival status. Median time (in years) to disease progression was defined as the time interval between initial presentation (presence of tumor seen radiographically or on physical examination) and the first instance of tumor recurrence or distant metastases after initial surgical resection and/or chemoradiation therapy with radiographically negative evidence of residual tumor.

RESULTS

Clinicoradiologic summary

Of the 8 patients with MPLPS, 5 were female and 3 were male with a median age of 32 years old (range 10–68) at diagnosis. The

primary tumor site was mediastinum: 3 in the anterior mediastinum, of which 2 showed involvement/invasion of the pleura and anterior chest wall, as well as compression of the large vessels (superior vena cava, aortic arch, etc); 4 in the posterior mediastinum and paraspinal locations: 1 showed infiltration of the vertebral body with spinal cord impingement, 1 extended from left inferior pulmonary vein to upper lower retroperitoneum with encasement of lower thoracic aorta and renal artery. In one patient, the tumor was located at the orbital floor with invasion of orbital structures. Radiographically, the tumors showed heterogeneously low attenuation on computed tomography (CT) imaging (Fig. 1A, B), heterogeneous enhancement on positron emission tomography (PET), and heterogenous signal intensity with predominantly fatty signal characteristics and poorly defined borders on magnetic resonance imaging (MRI). The tumor ranged from 4.8–18.0 cm in greatest dimension (median 12.5 cm). The clinicopathologic data is summarized in Table 1.

Histopathologic features

Majority of the MPLPS cases (7 of 8, 88%) presented as large mediastinal masses with involvement of adjacent structures, most commonly chest wall (Fig. 1C, E), pleura and lungs (Fig. 1D, F), and other mediastinal structures, such as the pericardium, diaphragm, large vessels, and spine. Grossly, MPLPS was multilobated with a heterogenous cut surface ranging from yellowish fat-like to myxoid/gelatinous (Fig. 1C) or tan-white to pink, fleshy and firm (Fig. 1D). At scanning power, MPLPS often demonstrated alternating hypo- and hypercellular nodules (Fig. 1G) (63%), corresponding to juxtaposition of myxoid, MRLPS-like areas that ranged from paucicellular to cellular round cell areas, and lipogenic, PLPS-like areas with epithelioid cells (Fig. 1H).

The predominant histopathologic feature (100%) was the presence of plexiform or chicken-wire vascular network intimately admixed with univacuolated or signet ring lipoblasts characteristically seen in MRLPS (Fig. 2A) and/or multivacuolated, pleomorphic lipoblasts with hyperchromatic, indented nuclei typically seen in PLPS (Fig. 2B, C). In three cases (cases 2, 6 and 8) (38%), the pleomorphic lipoblasts demonstrated xanthoma-like foamy cytoplasm (Fig. 2D, E). Classic, “pulmonary edema”-like cystic spaces with myxoid pools characteristic of MRLPS were also seen (Fig. 2F) in at least one case (13%). In at least two cases (25%), there were paucicellular lipoma-like areas with thin fibrous septa containing scattered hyperchromatic, atypical cells, reminiscent of well-differentiated liposarcoma (Fig. 2G). In six cases (cases 1, 2, 3, 5, 7 and 8) (75%), conspicuous mitotic activity (>10 per 10 high power fields) was present. In four cases (cases 1, 2, 7 and 8) (50%), tumor necrosis (focal to large confluent areas) was seen. Solid areas of epithelioid to spindled cells with severe cytologic atypia admixed with sheets of pleomorphic or signet ring-like lipoblasts or were identified in 5 cases (cases 1, 2, 3, 7 and 8) (63%). Interestingly, case 1 demonstrated lipogenic areas (Fig. 2H) that transitioned abruptly to solid, non-lipogenic and hypercellular, undifferentiated pleomorphic sarcoma-like areas with severe cytologic atypia, which was reminiscent of a dedifferentiated LPS, and raised the possibility of a similar phenomenon of dedifferentiation occurring in MPLPS (Fig. 2I).

Mutational and whole gene copy number alterations

All 8 (100%) MPLPS cases harbored *TP53* mutations (3 splice site, 1 frameshift, 2 nonsense and 2 missense mutations). Six out of the 7 *TP53* mutations had a variant allele frequency (VAF) > 0.5, indicating LOH at the *TP53* locus (Fig. 3A, Table 2). The only other recurrent gene level alterations were *EP300* mutations, amplification of *MYC*, *CEBPA* and *CCNE1* and deletion of *RB1* (2 cases each) (Fig. 3A). None of the MPLPS cases had a documented history of germline predisposition, including Li-Fraumeni syndrome.

In comparison, among 23 cases of PLPS, which also showed recurrent *TP53* mutations (83%), *RB1* deletion and *ATRX* alterations

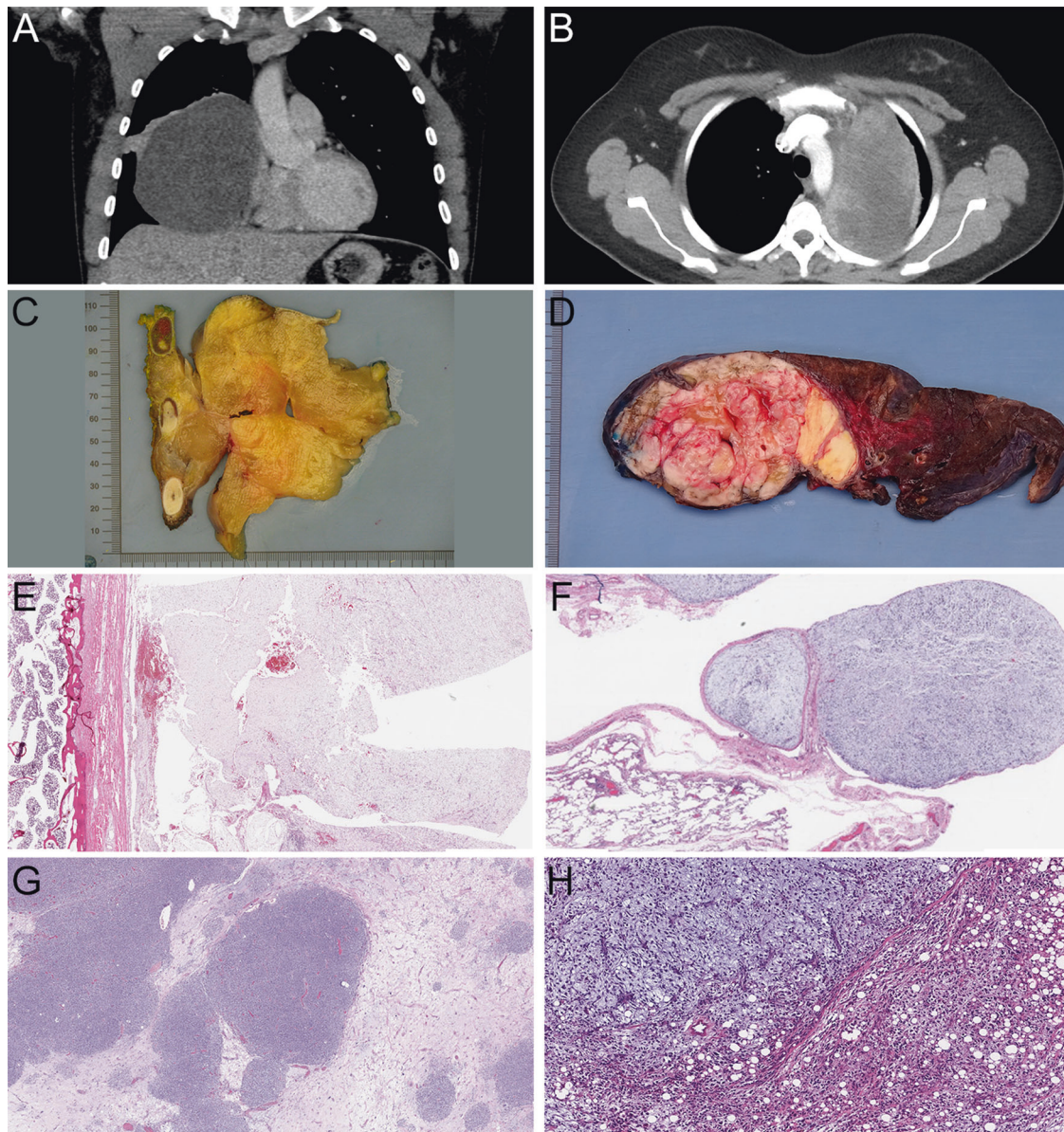


Fig. 1 Radiologic, gross pathologic and histologic features of myxoid pleomorphic liposarcoma. **A** Coronal chest computed tomography (CT) showing a large pleural-based soft tissue mass involving the right anterior mediastinum, chest wall and pericardium (case 5). **B** showing paramediastinal mass involving the left upper lung lobe (case 7). **C** Gross pathology specimen showing a large fatty, multilobated tumor invading the rib cage (case 5). **D** Gross pathology specimen showing a tan-white to pink, fleshy, and multiloculated mass adherent to the pleura and lung surface (case 7). **E** Low power photomicrograph showing a multilobated myxoid tumor adherent to the pleura with adjacent lung parenchyma (case 7, 2×). **F** Low power photomicrograph showing a multilobated myxoid tumor involving bone (chest wall) (case 5, 2×). **G** Intermediate power showing alternative hypo- and hypercellular nodules (case 7, 10×). **H** Intermediate power showing juxtaposition of myxoid liposarcoma-like area with myxoid stroma (upper left) and plexiform vasculature and lipogenic pleomorphic liposarcoma like cellular area (lower right) (case 4, 100×). **E–H** Hematoxylin & eosin stain.

were more common (48% and 39% respectively) (Fig. 3A, B). The 34 cases of MRLPS, all molecularly confirmed to harbor *DDIT3* gene rearrangement, were highly enriched in *TERT* 5' promoter mutations (88%) and mutations involving the PI3K/AKT pathway, most commonly *PIK3CA* (38%) and *PTEN* (29%) (Fig. 3A, C). The distribution of gene alterations in MRLPS did not differ between low-grade and high-grade tumors (Supplementary Fig. 1).

Across all three liposarcoma subtypes, *TERT* was mutually exclusive with *TP53*, *RB1* and *ATRX* alterations. *TP53* tended to co-occur with *RB1* and *ATRX* but was mutually exclusive with *PIK3CA* and *PTEN*, the latter two genes tended to co-occur with each other despite being involved in the same pathway (Supplementary Fig. 2).

Allele-specific copy number profile

Copy number profiling revealed multiple chromosomal arm level gains (as indicated by total copy numbers) and specifically, recurrent amplifications of chromosomes 1, 19 and 21 (Fig. 4A, B). On a cohort level, copy number gains but not losses were the predominant feature.

Importantly, allelic imbalance analysis by FACETS revealed widespread loss of heterozygosity (LOH), affecting on average 80% (mean) (range: 64–100%) of the genome in MPLPS, but not in PLPS [mean 38% LOH (range 20–66%)] or MRLPS [mean 5% LOH (range 0–17%)], as indicated by the non-zero and elevated allelic log-odds-ratios and a minor copy number (lcn) of 0 (Figs. 5A, 6A–E, Supplementary Figs. 3–5). A near-haploid state

Table 1. Clinical summary and follow-up.

Case	Age (y)/Sex	Primary site	Size (cm)	Initial Resection Margin Status	Recurrence/ Metastasis	Treatment	Outcome	Follow-up period (months)
1	62/M	Anterior mediastinum	12.90	Negative	Chest wall (local recurrence)	Neoadjuvant gemcitabine/ docetaxel, surgical resection, AIM, doxorubicin, nivolumab/ ipilimumab	AWD	52
2	24/F	Posterior/paraspinal mediastinum	18.00	Positive	T1-T3 spine metastases	Surgical resection, AIM	DOD	15
3	68/F	Paraesophageal mass	12.00	Positive	Pleural & lung (local recurrence)	Surgical resection, gemcitabine, docetaxel, olaratumab	DOD	21
4	52/F	Posterior/paraspinal mediastinum centered at T3-T4 and borders aortic arch, esophagus, vertebra and ribs	17.50	Negative	Pleural & lung (local recurrence)	Surgical resection, eribulin, docetaxel/gemcitabine, pazopanib	AWD	49
5	30/M	Anterior mediastinal pleural-based mass involving right supradiaphragmatic fat and invading right anterior chest wall, compressing superior vena cava and right atrium	13.50	Positive	Kidney metastasis	Surgical resection, unknown	AWD	14
6	10/M	Orbital Floor	4.80	N/A	Femur & liver metastases	Ifosfamide, eribulin, radiation therapy, doxorubicin, olaratumab	DOD	22
7	34/M	Left upper lung lobe paramediastinal mass	8.00	Negative	Pleural & paraspinal (local recurrence)	Neoadjuvant AIM, resection, eribulin, trabectedin	DOD	14
8	22/F	Posterior lower mediastinum extending from left inferior pulmonary vein to upper left retroperitoneum, encasing lower thoracic aorta and renal artery	11.40	Positive	Sacrum and T8 epidural metastases	Neoadjuvant AIM and radiation therapy, surgical resection, doxorubicin, dacarbazine, eribulin	DOD	52

AIM doxorubicin, ifosfamide, mesna, AWD alive with disease, DOD died of disease.

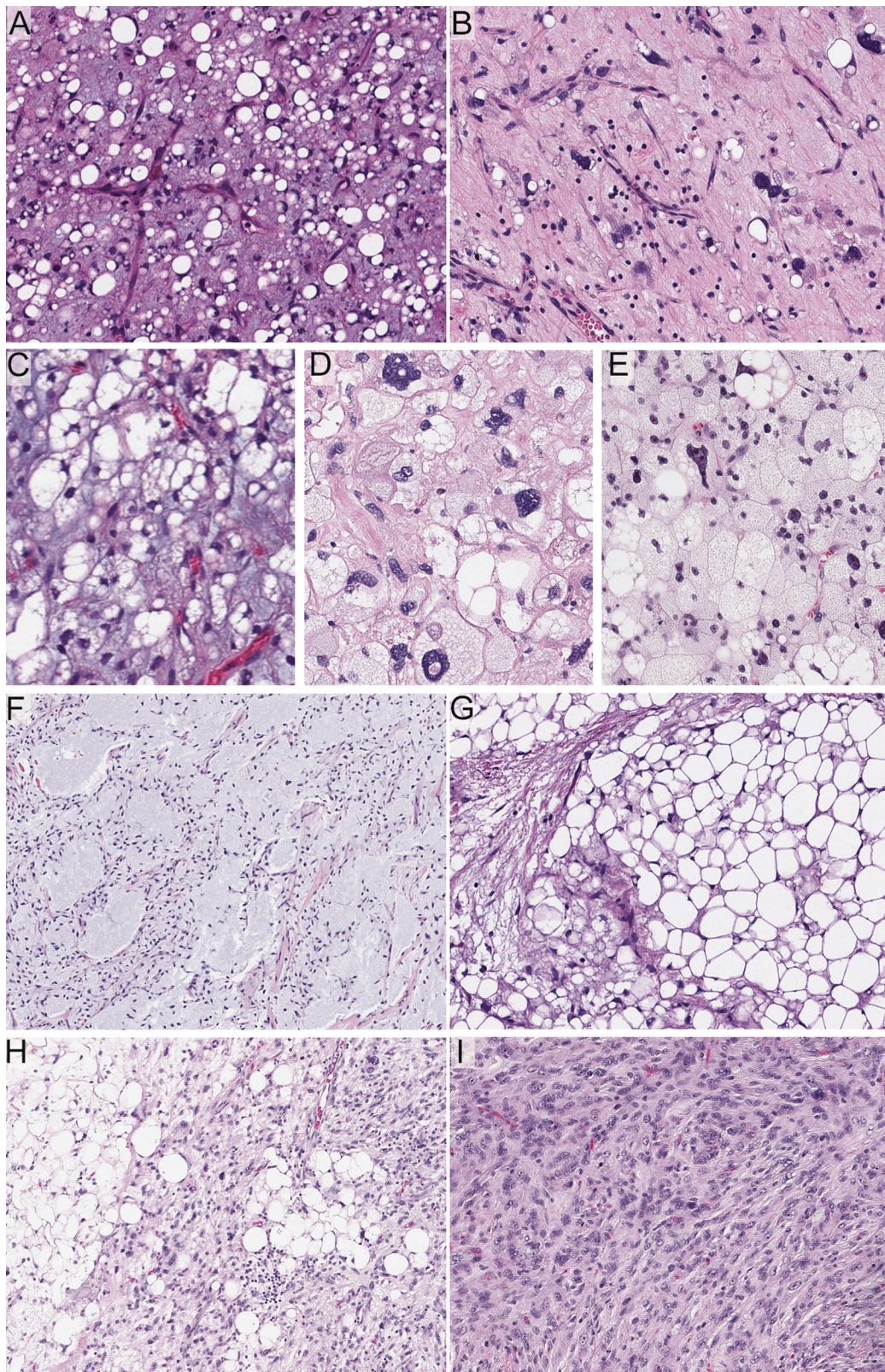


Fig. 2 Histopathologic features of myxoid pleomorphic liposarcoma (MPLPS). MPLPS is characterized by chicken wire-like vasculature seen in myxoid/round cell liposarcoma (MRLPS) admixed with univacuolated signet ring-like lipoblasts in MRLPS (A) or multivacuolated pleomorphic lipoblasts typically seen in PLPS (B, C) (A case 3, 100x. B case 7: 200x. C case 2: 200x). In some cases, the pleomorphic lipoblasts demonstrate foamy cytoplasm (xanthoma-like) (D case 8, 400x. E case 6, 200x). Classic, “pulmonary edema”-like cystic spaces characteristic of MRLPS could be seen in MPLPS (F case 5, 100x). Occasionally, paucicellular lipogenic areas reminiscent of well-differentiated liposarcoma could be seen (G case 3, 100x). Case 1 also demonstrated lipogenic but highly cellular areas with high-grade nuclear atypia (H 200x) that transitions abruptly to non-lipogenic and cellular, undifferentiated pleomorphic sarcoma-like areas (I 200x), suggesting a “dedifferentiated” process.

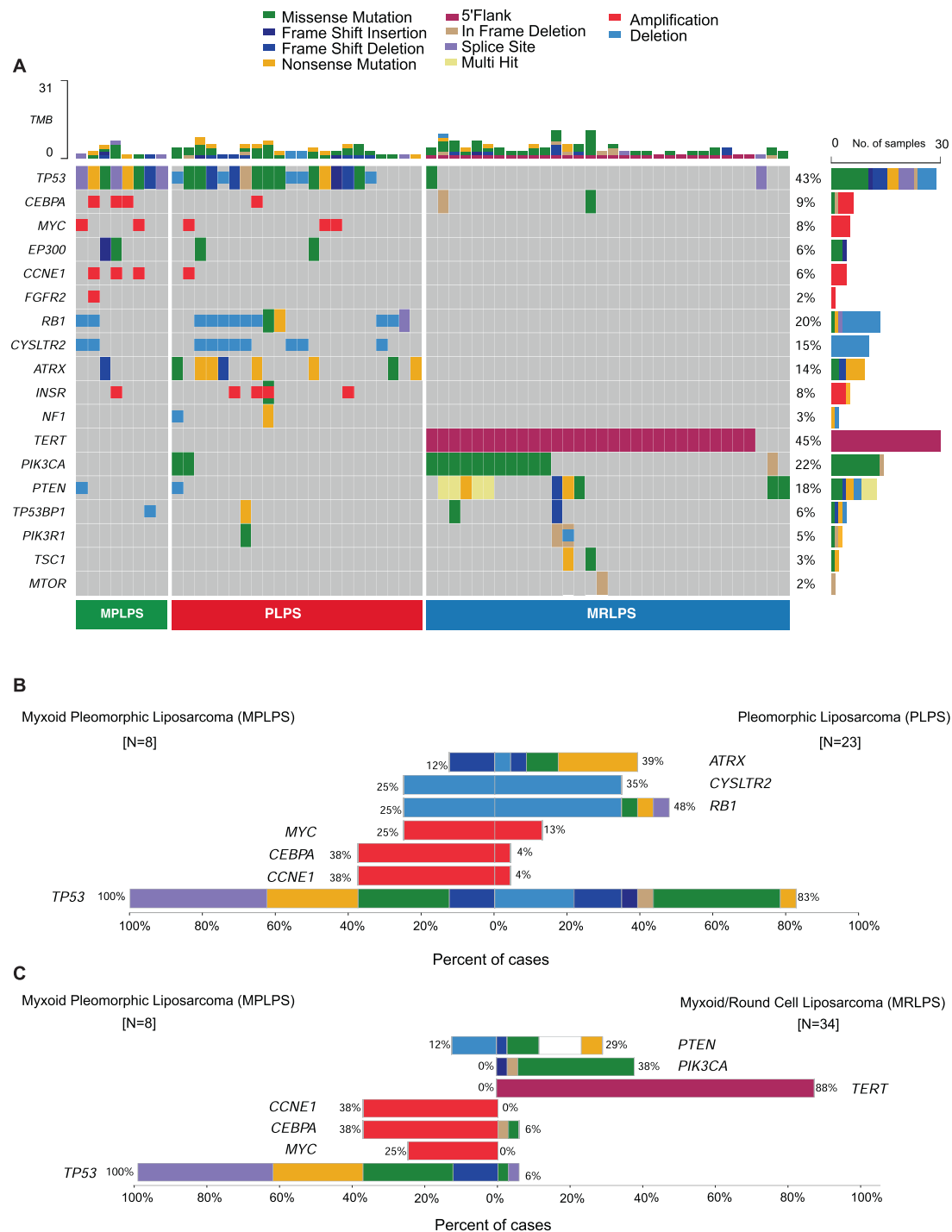


Fig. 3 Recurrent gene-level mutations and copy number alterations across different liposarcoma subtypes. **A** OncoPrint showing recurrent gene mutations and copy number alterations in myxoid pleomorphic liposarcoma (MPLPS), pleomorphic liposarcoma (PLPS), and myxoid/round cell liposarcoma (MRLPS). TMB tumor mutation burden (unit mutations/megabase). **B** Co-bar plots comparing the mutational frequencies of recurring genetic alterations between MPLPS and PLPS. **C** Co-bar plots comparing the mutational frequencies of recurring genetic alterations between MPLPS and MRLPS.

was evident in two of the copy number plots (Fig. 5A) where the total copy number (tcn) was 1 and lcn was 0 for most of the chromosomes. In the remaining cases, while the lcn was zero, the tcn was 2 or greater, resulting in a hyperdiploid state likely derived from doubling of a near-haploid genome. Interestingly,

the metastatic tumor of one of these two cases with near-haploid genome also underwent MSK-IMPACT sequencing, and showed a mostly diploid genome, supporting the theory of whole genome doubling of the original primary tumor (Fig. 4A).

Table 2. Molecular testing summary of the MPLPS cohort.

Case	MDM2 and CDK4	DDIT3 rearrangement	Archer testing	TP53 mutation	TP53 VAF
1	Negative by IHC	FISH not performed	Not performed	c.524 G > A (p.R175H)	0.67
2	Negative for amplification by FISH	FISH not performed	Not performed	c.577 C > T (p.H193Y)	0.74
3	Negative by IHC	Negative by FISH	Negative for gene fusions	c.949 C > T (p.Q317*)	0.28
4	Negative for amplification by FISH	Negative by FISH	Negative for gene fusions	c.376-8_384del (p.X126_splice)	0.94
5	Negative for amplification by FISH	Negative by FISH	Negative for gene fusions	c.642_643delTA (p.H214Qfs*7)	0.94
6	Not tested	Negative by FISH	Not performed	c.994-1 G > C (p.X332_splice)	0.41
7	Negative by IHC	Negative by FISH	Negative for gene fusions	c.376-1 G > T (p.X126_splice)	0.80
8	Both MDM2/CDK4 and centromere 12 amplified	FISH not performed	Negative for gene fusions	c.637 C > T (p.R213*)	0.78

FISH fluorescence in situ hybridization, IHC immunohistochemistry, TP53 (NM_000546), VAF variant allele frequency.

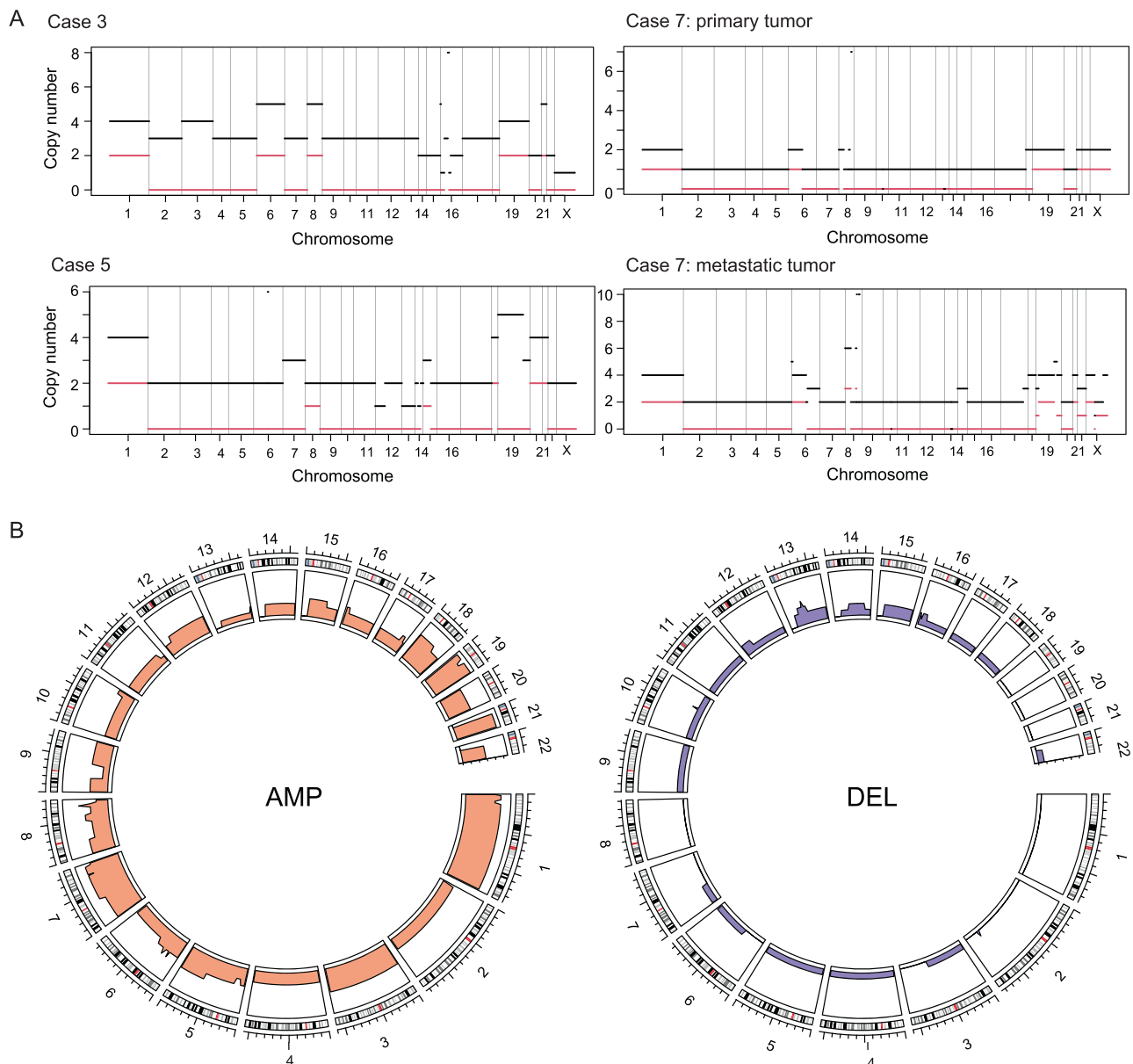


Fig. 4 Genome-wide copy number alterations in myxoid pleomorphic liposarcoma. **A** Individual copy number plots across chromosomes 1 through 22 and X from four representative cases. Horizontal black lines represent total copy number. Horizontal red lines represent minor copy number for each segment. Expectation-maximization algorithm applied for integer copy number call¹¹. **B** Circos genomic plots with cytoband data representing cohort level ($n = 7$) total copy numbers across chromosomes 1 through 22 (AMP amplification, DEL deletion).

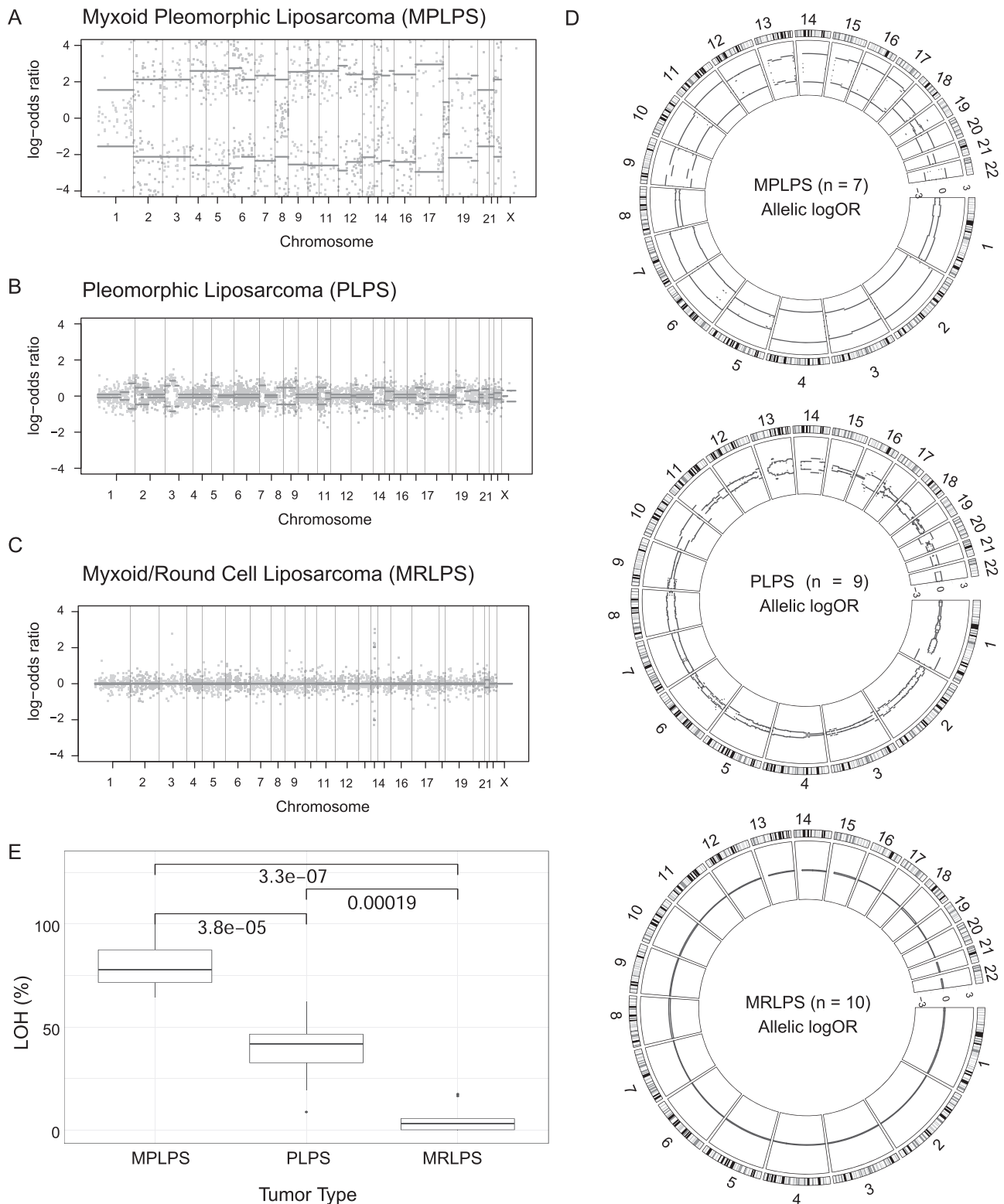


Fig. 5 Widespread loss of heterozygosity in myxoid pleomorphic liposarcoma (MPLPS). Representative allelic log-odds-ratio (logOR) plots of MPLPS (A), pleomorphic liposarcoma (PLPS) (B), and myxoid/round cell liposarcoma (MRLPS) (C) generated by FACETS. Segment means are plotted in red lines. D Cohort level logOR represented by median logOR values on circo genomic plots with cytoband data across all samples in MPLPS (n = 7), PLPS (n = 9), MRLPS (n = 10), respectively. E Boxplots comparing the percentages of loss of heterozygosity (LOH) across the genome among MPLPS, PLPS and MRLPS. Center line corresponds to the median; lower and upper hinges correspond to 25th and 75th percentiles; upper and lower whiskers correspond to 1.5× inter-quartile range. Numbers between sample groups represent adjusted *p*-values by pairwise analysis (method = Benjamini-Hochberg, BH).

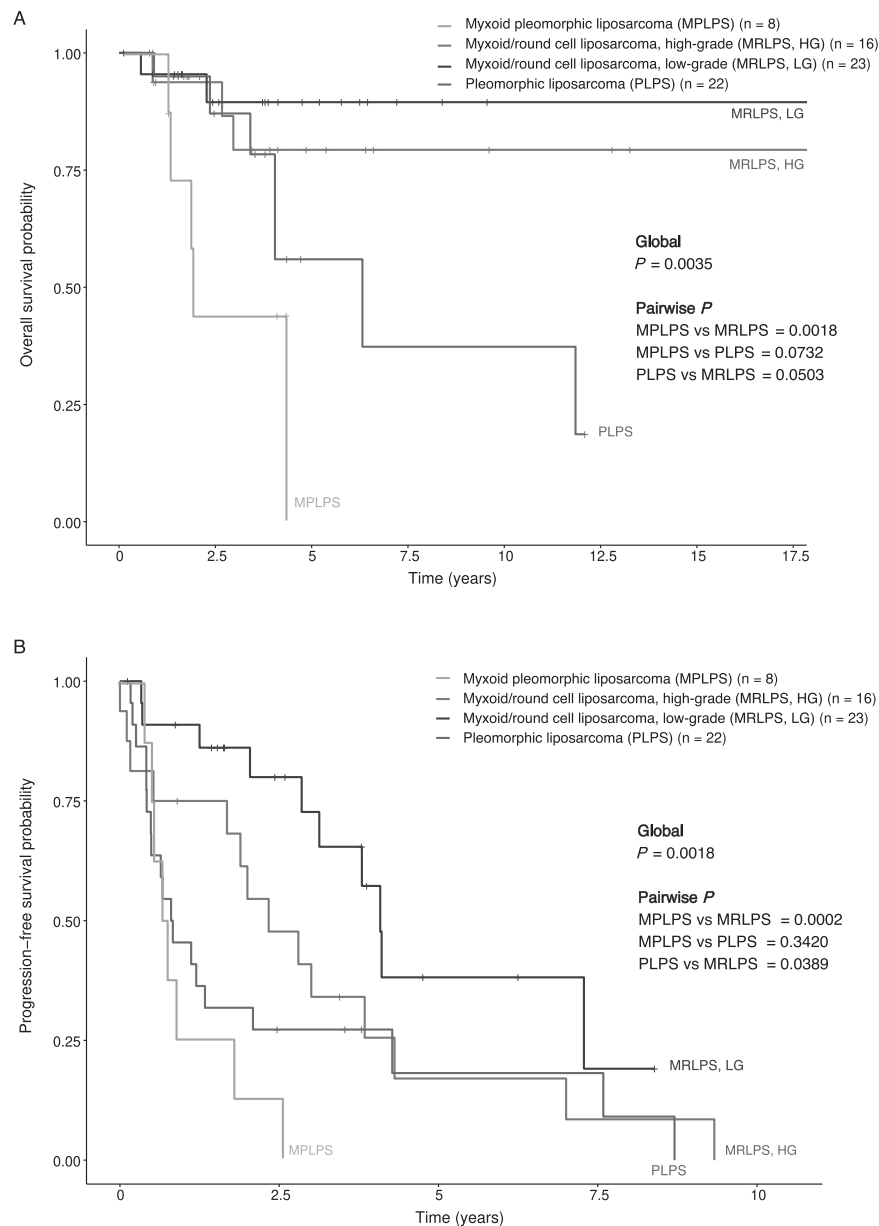


Fig. 6 Overall and progression-free survival among different liposarcoma subtypes. Kaplan-Meier survival curves of myxoid pleomorphic liposarcoma (MPLPS), pleomorphic liposarcoma (PLPS), and myxoid/round cell liposarcoma (MRLPS) (high grade and low grade): **A** overall survival, **B** progression-free survival. P -values based on log-rank test, including global p -values and adjusted p -values by pairwise analysis (method = Benjamin-Hockberg, BH).

Outcome and survival

In terms of treatment, all except one patient who received radiation and chemotherapy underwent surgical resection. The chemotherapy regimens included adriamycin, ifosfamide + mesna (AIM), gemcitabine plus docetaxel, eribulin, doxorubicin, with or without olaratumab, pazopanib, nivolumab or trabectedin. All patients showed disease progression: 4 with local recurrence in (chest wall, pleura, lung, mediastinum) and 4 with distant metastasis (kidney, liver, spine, femur). Five patients died of disease. Median follow-up period was 22 months (range 14–52 months) (Table 1).

Importantly, compared to PLPS and MRLPS (high-grade and low-grade), the overall survival ($P = 0.0035$) and progression-free survival ($P = 0.0018$) in MPLPS were significantly worse (Fig. 6A, B). Median time to progression for MPLPS was 8.7 months, compared to 9.8 and 45.6 months for PLPS and MRLPS, respectively. Median

time to death for MPLPS was 22.6 months, compared to 75.9 and 218.3 months for PLPS and MRLPS, respectively.

DISCUSSION

In this study, we performed comprehensive genomic profiling of MPLPS in comparison with pleomorphic liposarcoma PLPS and MRLPS. The patients from our case series with MPLPS had a broad age range of 10–68 with a median age of 32 years old, which is consistent with the recent report of 12 cases by Creyten et al that had a range of 17–58 years and a median age of 35 years old³. Our gender distribution was 5 females and 3 males. The 12 cases reported by Creyten et al. showed an equal sex ratio. Overall, based on the reported cases in the literature (summarized in Table 3), the mean and median ages reported in all 38 cases reported thus far were 29 and 22.5 years old, with a range of 5–68

Table 3. Literature review of myxoid pleomorphic liposarcoma.

Author (year)	# cases	Age in years (range, mean/median)	Sex	Location	Molecular Assays	Molecular Alterations	Outcome
Plukker 1988	1	5	Male	Mediastinum	None	N/A	DOD 17 months after diagnosis. Recurrence at 10 months after surgical resection and chemotherapy.
Greif 1998	1	62	Male	Mediastinum	None	N/A	DOD 2 years after diagnosis. Recurrence 8 months after surgical resection and radiation therapy.
Alaggio 2009	12	10–22 (mean 16, median 17)	8 females, 4 males	Mediastinum (5), thigh (3), trunk (2), retroperitoneum (1), head (1)	FISH	No <i>MDM2</i> gains or <i>DDIT3</i> rearrangement	6 DOD in 8 months to 3 years. 2 ANED after 5 and 8 years. 1 AWD at 3 years with distal metastases. 3 no follow-up.
Boland 2012	3	23, 48, 62	1 female, 2 males	Mediastinum (3)	FISH	No <i>MDM2</i> gains or <i>DDIT3</i> rearrangement	1 DOD after 15 months with recurrence and pleural metastases. 2 AWD at 9- and 36-month follow-up.
Creytens 2014	1	21	Male	Neck	Array-based comparative genomic hybridization (CGH)	Gains in chr 1q, 6–8, 19–21, X, losses in chr 2–5, 10–17, 22	N/A
Hofvander 2015	1	10	Male	Medial left thigh	Karyotyping, SNP array, whole exome, targeted, and RNA-sequencing	<i>R81</i> loss, hyperdiploid/hypotriploid karyotype with near haploidization, <i>KMT2D</i> frameshift deletion	ANED after surgical resection and adjuvant chemotherapy (follow-up period uncertain)
Creytens 2021	12	17–58 (mean 33, median 35)	6 females, 6 males	Mediastinum (5), back (1), neck (2), cheek (1), leg (3), including 2 thighs	FISH, genome-wide copy number profiling, methylation profiling	Gains in chr 1, 6–8, 18–21, losses in chr 13 (including <i>R81</i> , <i>RCTB2</i> , <i>DLEU1</i> , <i>ITM2B</i>), 16, 17	Metastases and DOD within 40 months in all patients with available clinical follow-up
Current study	8	10–68 (mean 38, median 32)	5 females, 3 males	Mediastinum (7), orbit (1)	Targeted DNA sequencing (MSK-IMPACT), FISH, Archer	<i>TP53</i> mutations, recurrent gains in chr 1, 19, 21, genome-wide loss of heterozygosity (near-haploidization)	Local recurrence/metastases in all patients (median time 8.7 months. 5 DOD (median survival 22.6 months)
Overall	39	5–68 (mean 29, median 23)	20 females, 19 males	Mediastinum (22), thigh (6), trunk (3), head (3), neck (3), leg (1), retroperitoneum (1)			26 DOD, 6 AWD, 3 ANED, 4 no follow-up

ANED alive with no evidence of disease, AWD alive with disease, DOD died of disease.

years old, and a 1:1 female-to-male ratio. This suggests that MPLPS is not limited to young adults only and may show a balanced gender distribution rather than a true female predominance that was previously described^{1,3}.

Nevertheless, similar to prior reports, in our cohort MPLPS followed a highly aggressive clinical course, with a 100% progression rate in the form of either local recurrence or distant metastasis. From our literature review of 35 cases with available clinical follow-up, 26 (74%) succumbed to disease within a few years (Table 3)^{1–5,12–14}. In our study, the median time to progression was extremely short: only 8.7 months, with a progression-free survival and overall survival that were worse compared to PLPS and markedly worse than MRLPS, including the high-grade variant. In our MPLPS cohort, the patients underwent standard clinical management for advanced soft tissue sarcomas, primarily surgical resection with or without radiation and neoadjuvant or adjuvant chemotherapy regimens using drugs that had shown efficacy in the treatment of liposarcomas: trabectedin and eribulin, as well as non-histotype-specific sarcoma regimens: AIM (doxorubicin, ifosfamide, mesna), gemcitabine and docetaxel, etc.^{15,16}. Nonetheless, despite aggressive treatment, all patients in our limited cohort experienced rapid disease progression. We speculate that the clinical aggressiveness of this entity is related to its mediastinal location, large size and invasion of vital mediastinal structures, and the associated challenge in achieving complete surgical resection with clean margins.

Histopathologically, MPLPS is characterized by an admixture and variable proportions of MRLPS-like areas with a characteristic, delicate plexiform vasculature and uniform spindled to round cells, and high-grade PLPS-like areas with pleomorphic lipoblasts and severe cytological atypia. In MRLPS, which harbors *FUS::DDIT3* or *EWSR1::DDIT3* gene fusions (the latter of which being more common in the round cell/high grade variant)¹⁷, tumor cells demonstrate monotonous cytology: either uniformly bland ovoid-to-spindled cells or round cells with enlarged nuclei, with or without scattered univacuolated lipoblasts. Nuclear pleomorphism and pleomorphic lipoblasts should be absent. PLPS, on the other hand, predominantly demonstrates undifferentiated pleomorphic sarcoma (UPS)-like morphology: cellular sheets of obviously malignant cells with severe nuclear atypia and pleomorphism and scattered/clustered populations of multivacuolated pleomorphic lipoblasts. A subset of PLPS is known to demonstrate myxofibrosarcoma (MFS)-like areas¹⁸: myxoid areas containing coarse, curvilinear vasculature with “clinging” tumor cells and pleomorphic and atypical spindled cells, which is distinct from the lack of cellular pleomorphism and severe nuclear atypia in MRLPS.

In terms of mutational profiling, our findings validated the prior reports on the high frequency of *TERT* promoter mutations in MRLPS: 74% (29/39) in the study by Koelsche et al.¹⁹ compared to 88% (26/29) in our study. Consistent with their findings, the presence of *TERT* promoter mutations were not associated with tumor grade (myxoid vs round cell variant) in our study (Supplementary Fig. 1). Similarly, prior reports showed enrichment of mutations in genes involved in the PI3K/AKT pathway in MRLPS: 18% and 14% with *PIK3CA* mutations in the studies by Barretina et al and Demicco et al, respectively^{20–22}. Demicco et al also showed mutually exclusive *PTEN* loss in 12% of cases²¹. In our study, the frequencies of *PIK3CA* and *PTEN* mutations in MRLPS were even higher: 38% and 29% respectively. Interestingly, although *PIK3CA* and *PTEN* alterations were mutually exclusive in the study by Demicco et al.²¹, we found a substantial number of cases with cooccurrence of *PIK3CA* and *PTEN* alterations.

Among PLPS, we identified high frequencies of *TP53* mutations, *RB1* deletion, and complex copy number profiles, consistent with previous findings^{20,23}. Coincidentally, a case of perineal MPLPS was reported in a 15-year-old female with a germline pathogenic *TP53* mutation (Li-Fraumeni syndrome)²⁴. However, in contrast to prior reports^{3,5}, which showed *RB1* deletion in 1 out of 1 case and

4 out of 8 cases, respectively, our results showed only two out of 8 cases of MPLPS with *RB1* deletion. Nevertheless, we acknowledge that a targeted panel-based NGS approach can potentially miss *RB1* inactivating events, particularly large deletions or microdeletions not captured by the panel, which may be better detected by alternate approaches such as fluorescence in-situ hybridization (FISH), array comparative genomic hybridization (CGH) or single nucleotide polymorphism (SNP) arrays²⁵. Therefore, the frequency of *RB1* loss in MPLPS may have been underestimated in our series.

Given the lack of completely specific biomarkers for MPLPS, we intentionally excluded liposarcomas from the extremities, particularly the thighs, to avoid inadvertent inclusion of conventional PLPS in our MPLPS cohort. In our opinion, the distinction between PLPS with myxoid changes and MPLPS can be quite challenging by morphology alone, and we believe that consideration of clinical (particularly mediastinal location) and molecular findings is necessary to establish an accurate diagnosis of MPLPS. On the other hand, we identified recurrent *TP53* mutations in 8 out of 8 (100%) of our MPLPS cases, which has not been reported before in this tumor type to our knowledge. All in all, in our experience MPLPS was relatively genetically “quiet” in terms of mutations, compared to PLPS and MRLPS.

Additionally, the predominant chromosomal copy number alterations were amplification rather than losses, resulting in a hyperdiploid state. Importantly, we observed consistently widespread LOH among all 7 of the MPLPS cases with FACETS data not seen in PLPS or MRLPS. This phenomenon has only been reported in one case report of MPLPS using SNP array⁵. As FACETS utilized heterozygous SNPs in tumor and matched normal to assess allele-specific copy number changes, we were able to evaluate for the presence of LOH, total copy numbers, and minor (allele) copy numbers. We hypothesize this widespread, genome-wide LOH in an otherwise hyperdiploid genome to be similar to the near-haploidization phenomenon observed in inflammatory leiomyosarcoma (ILMS), also known as inflammatory rhabdomyoblastic tumor or “histiocyte-rich rhabdomyoblastic tumor”^{26–28}. Association with *TP53* mutation, however, has not been reported in ILMS. Whole genome doubling has been found in a pan-cancer study to predict for increased risk of death and to be near twice as common in *TP53*-mutant tumors. This was thought to be related to the biological role of intact *TP53* in the prevention of genome-doubled cells from reentering the cell cycle²⁹.

In summary, our findings suggest that widespread LOH (likely a result of doubling of a near-haploid genome) and recurrent *TP53* mutations represent characteristic genomic features that are specific to MPLPS compared to other liposarcoma subtypes, with MPLPS also associated with distinct clinicopathologic features and an aggressive outcome.

DATA AVAILABILITY

The raw data generated are not publicly available due to lack of access to indefinite hosting capabilities, but are available from the corresponding author on reasonable request.

REFERENCES

- Alaggio R., Coffin C.M., Weiss S.W., Bridge J.A., Issakov J., Oliveira A.M. & Folpe A.L. Liposarcomas in young patients: a study of 82 cases occurring in patients younger than 22 years of age. *Am. J. Surg. Pathol.* **33**, 645–658 (2009).
- Boland J.M., Colby T.V. & Folpe A.L. Liposarcomas of the mediastinum and thorax: a clinicopathologic and molecular cytogenetic study of 24 cases, emphasizing unusual and diverse histologic features. *Am. J. Surg. Pathol.* **36**, 1395–1403 (2012).
- Creytens D., Folpe A.L., Koelsche C., Mentzel T., Ferdinande L., van Gorp J.M., et al. Myxoid pleomorphic liposarcoma—a clinicopathologic, immunohistochemical, molecular genetic and epigenetic study of 12 cases, suggesting a possible relationship with conventional pleomorphic liposarcoma. *Mod. Pathol.* **34**, 2043–2049 (2021).

4. Creyten D., van Gorp J., Ferdinande L., Van Roy N. & Libbrecht L. Array-based comparative genomic hybridization analysis of a pleomorphic myxoid liposarcoma. *J. Clin. Pathol.* **67**, 834–835 (2014).
5. Hofvander J., Jo V.Y., Ghanei I., Gisselsson D., Mårtensson E. & Mertens F. Comprehensive genetic analysis of a paediatric pleomorphic myxoid liposarcoma reveals near-haploidization and loss of the RB1 gene. *Histopathology*. **69**, 141–147 (2016).
6. Cheng D.T., Mitchell T.N., Zehir A., Shah R.H., Benayed R., Syed A., et al. Memorial Sloan Kettering-Integrated Mutation Profiling of Actionable Cancer Targets (MSK-IMPACT): A Hybridization Capture-Based Next-Generation Sequencing Clinical Assay for Solid Tumor Molecular Oncology. *J. Mol. Diagn.* **17**, 251–264 (2015).
7. Mayakonda A., Lin D., Assenoy Y., Plass C. & Koeffler P.H. “Maftools: efficient and comprehensive analysis of somatic variants in cancer.” *Genome Res.* **28**, 1747–1756 (2018).
8. Zhang J. (2021). *CNTools: Convert segment data into a region by sample matrix to allow for other high level computational analyses*. R package version 1.50.0.
9. Wang, S., Li, H., Song, M., Tao, Z., Wu, T. & He, Z. et al. Copy number signature analysis tool and its application in prostate cancer reveals distinct mutational processes and clinical outcomes. *PLoS Genet* **17**, e1009557 (2021).
10. Gu, Z. Circlize implements and enhances circular visualization in R. *Bioinformatics*. **30**, 2811–2812 (2014).
11. Shen, R. & Seshan, V. E. FACETS: allele-specific copy number and clonal heterogeneity analysis tool for high-throughput DNA sequencing. *Nucleic Acids Res* **44**, e131 (2016).
12. Plukker, J.T., Joosten, H.J., Rensing, J.B. & Van Haelst U.J. Primary liposarcoma of the mediastinum in a child. *J. Surg. Oncol.* **37**, 257–263 (1988).
13. Greif J., Marmor S., Merimsky O., Kovner F. & Inbar M. Primary liposarcoma of the mediastinum. *Sarcoma*. **2**, 205–257 (1998).
14. Hahn H.P. & Fletcher C.D. Primary mediastinal liposarcoma: clinicopathologic analysis of 24 cases. *Am. J. Surg. Pathol.* **31**, 1868–1874 (2007).
15. von Mehren M., Randall R.L., Benjamin R.S., Boles S., Bui M.M., Ganjoo K.N., et al. Soft Tissue Sarcoma, Version 2.2018, NCCN Clinical Practice Guidelines in Oncology. *J. Natl. Compr. Canc. Netw.* **16**, 536–563 (2018).
16. Gronchi A., Miah A.B., Dei Tos A.P., Abecassis N., Bajpai J., Bauer S., Biagini R., et al. Soft tissue and visceral sarcomas: ESMO-EURACAN-GENTURIS Clinical Practice Guidelines for diagnosis, treatment and follow-up. *Ann. Oncol.* **32**, 1348–1365 (2021).
17. Bode-Lesniewska B., Frigerio S., Exner U., Abdou M.T., Moch H. & Zimmermann DR. Relevance of translocation type in myxoid liposarcoma and identification of a novel EWSR1-DDIT3 fusion. *Genes Chromosomes Cancer*. **46**, 961–971 (2007).
18. Hornick J.L., Bosenberg M.W., Mentzel T., McMenamin M.E., Oliveira A.M. & Fletcher C.D. Pleomorphic liposarcoma: clinicopathologic analysis of 57 cases. *Am. J. Surg. Pathol.* **28**, 1257–1267 (2004).
19. Koelsche C., Renner M., Hartmann W., Brandt R., Lehner B., Waldburger N., et al. TERT promoter hotspot mutations are recurrent in myxoid liposarcomas but rare in other soft tissue sarcoma entities. *J. Exp. Clin. Cancer Res.* **33**, 33 (2014).
20. Barretina J., Taylor B.S., Banerji S., Ramos A.H., Lagos-Quintana M., Decarolis P.L., et al. Subtype-specific genomic alterations define new targets for soft-tissue sarcoma therapy. *Nat. Genet.* **42**, 715–721 (2010).
21. Demicco E.G., Torres K.E., Ghadimi M.P., Colombo C., Bolshakov S., Hoffman A., et al. Involvement of the PI3K/Akt pathway in myxoid/round cell liposarcoma. *Mod. Pathol.* **25**, 212–221 (2012).
22. Trautmann M., Cyra M., Isfort I., Jeiler B., Krüger A., Grünwald I., et al. Phosphatidylinositol-3-kinase (PI3K)/Akt Signaling is Functionally Essential in Myxoid Liposarcoma. *Mol. Cancer Ther.* **18**, 834–844 (2019).
23. Ghadimi M.P., Liu P., Peng T., Bolshakov S., Young E.D., Torres K.E., et al. Pleomorphic liposarcoma: clinical observations and molecular variables. *Cancer*. **117**, 5359–5369 (2011).
24. Sinclair T.J., Thorson CM., Alvarez E., Tan S., Spunt S.L. & Chao S.D. Pleomorphic myxoid liposarcoma in an adolescent with Li-Fraumeni syndrome. *Pediatr. Surg. Int.* **33**, 631–635 (2017).
25. Yoshikawa Y., Emi M., Hashimoto-Tamaoki T., Ohmura M., Sato A., Tsujimura T., et al. High-density array-CGH with targeted NGS unmask multiple noncontiguous minute deletions on chromosome 3p21 in mesothelioma. *Proc. Natl. Acad. Sci. U. S. A.* **113**, 13432–13437 (2016).
26. Dal Cin P., Sciot R., Fletcher C.D., Samson I., De Vos R., Mandahl N., et al. Inflammatory leiomyosarcoma may be characterized by specific near-haploid chromosome changes. *J. Pathol.* **185**, 112–115 (1998).
27. Arbajian E., Köster J., Vult von Steyern F. & Mertens F. Inflammatory leiomyosarcoma is a distinct tumor characterized by near-haploidization, few somatic mutations, and a primitive myogenic gene expression signature. *Mod. Pathol.* **31**, 93–100 (2018).
28. Cloutier J.M., Charville G.W., Mertens F., Sukov W., Fritch K., Perry K.D., et al. “Inflammatory Leiomyosarcoma” and “Histiocyte-rich Rhabdomyoblastic Tumor”: a clinicopathological, immunohistochemical and genetic study of 13 cases, with a proposal for reclassification as “Inflammatory Rhabdomyoblastic Tumor”. *Mod Pathol.* **34**, 758–769 (2021).
29. Bielski C.M., Zehir A., Penson A.V., Donoghue M.T.A., Chatila W., Armenia J., et al. Genome doubling shapes the evolution and prognosis of advanced cancers. *Nat. Genet.* **50**, 1189–1195 (2018).

ACKNOWLEDGEMENTS

We gratefully acknowledge the members of the Molecular Diagnostics Service in the Department of Pathology and would like to acknowledge the Center Core grant (P30 CA008748) and the Marie-Josée and Henry R. Kravis Center for Molecular Oncology for use of MSK-IMPACT data. This work was supported by P50 CA217694 (SS, WT, CRA), P30 CA008748 (SS, WT, CRA), Kristin Ann Carr Foundation (CRA). All other authors report no funding sources related to this study.

AUTHOR CONTRIBUTIONS

J.K.D performed study design, data acquisition, data analysis and interpretation, writing and revision of the paper. SCH, L.W., W.D.T., S.S. performed acquisition, analysis, and/or interpretation of data, and review of the paper. C.M.V. and C.R.A. performed study design and conception, analysis and interpretation of data, writing, review and revision of paper. All authors read and approved the final manuscript.

COMPETING INTERESTS

The authors declare no competing interests.

ETHICS APPROVAL/CONSENT TO PARTICIPATE

This study was approved by the Memorial Sloan Kettering Cancer Institute Institutional Review Board.

ADDITIONAL INFORMATION

Supplementary information The online version contains supplementary material available at <https://doi.org/10.1038/s41379-022-01107-6>.

Correspondence and requests for materials should be addressed to Cristina R. Antonescu.

Reprints and permission information is available at <http://www.nature.com/reprints>

Publisher's note Springer Nature remains neutral with regard to jurisdictional claims in published maps and institutional affiliations.